www.crt-journal.org

Crystal Research and Technology

Journal of Experimental and Industrial Crystallography
Zeitschrift für experimentelle und technische Kristallographie

WILEY-VCH

Cryst. Res. Technol. **47,** No. 9, 997–1003 (2012) / **DOI** 10.1002/crat.201200058

Controllable synthesis of hierarchical strontium molybdate by sonochemical method

Wanquan Jiang*[1], Wei Zhu[1], Chao Peng[2], Fan Yang[2], Shouhu Xuan[2], and Xinglong Gong[2]

[1] Department of Chemistry, University of Science and Technology of China (USTC), Hefei 230026, P. R. China
[2] CAS Key Laboratory of Mechanical Behavior and Design of Materials, Department of Modern Mechanics, USTC, Hefei 230027, P. R. China

Received 3 February 2012, revised 7 June 2012, accepted 8 June 2012
Published online 2 July 2012

Key words sonochemical, hierarchical structure, $SrMoO_4$.

Large-scale chrysanthemum-like strontium molybdate ($SrMoO_4$) with hierarchical structure has been successfully synthesized via a facile and fast ultrasound irradiation approach at room temperature. By varying the experimental conditions, $SrMoO_4$ with different morphologies, such as spindles, peanuts, spheres, and rods, can be obtained. The products are characterized by X-ray diffraction (XRD), scanning electron microscopy (SEM), transmission electron microscopy (TEM), and selected-area electron diffraction (SAED). The influent parameters including concentration, pH value, and surfactants have been investigated. A possible growth mechanism is proposed and the shape evolution of the products is characterized. The as-prepared chrysanthemum-like $SrMoO_4$ particles are used as the precursor for electrorheological fluid and their electrorheological property is investigated.

1 Introduction

Molybdates have wide applications in various areas, sucha as scintillation detector, solidstate optical maser, optical fiber, magnetic material, catalyst, light emitting diode, Raman laser and so on [1–8]. Among them, strontium molybdate ($SrMoO_4$) have attracted a great deal of interests due to their unique luminescence and structural properties. $SrMoO_4$ has body-centered tetragonal scheelite structure and the Mo atoms are surrounded by four equivalent O atoms in tetrahedral configuration and the divalent metals share corners with eight adjacent $[MoO_4]^{2-}$ tetrahedrons [9]. Because of the special crystal structure, $SrMoO_4$ exhibits excellent green and blue luminescent properties under liquid nitrogen temperature, which enable it use as efficient low-temperature scintillators for nuclear instrumental applications.

Due to their unique shape-dependent properties, great effort has been devoted to the morphology controlled synthesis of self-assembled hierarchical structures of molybdates with well-defined shapes. Recently, a variety of efficient techniques have been carried out on the shape-controlled $SrMoO_4$ crystal and different morphologies, such as particles, sheets, dumbbells, have been successfully prepared. Sun [10] synthesized $SrMoO_4$ rose-like and persimmon-like structures were synthesized via microwave radiation-assisted chelating agent method. Mi [11] developed a reverse microemulsion approach to synthesize 2D plate-like $SrMoO_4$ and the as-prepared $SrMoO_4$ nanoplates exhibited unique luminescent properties. Sun [12] obtained $CaMoO_4$ crystallites with different morphology by ethylene glycol-assisted electrochemical method. In this work, the photoluminescent property of $CaMoO_4$ crystallites can be controlled by varying experimental conditions. Therefore, the morphology controllable fabrication is very important for material designation.

Sonochemical method has become an ideal approach to synthesize materials with controlled morphologies. When ultrasound was act on liquid, acoustic cavitation occurred and generates localized hot spots having very high temperatures (>5000 K), pressures (>20 MPa), and cooling rates (>107 K/s) [13]. Such extreme environments provide a unique platform for the growth of novel nanostructures. Using this efficient and convenient process, many materials such as CdSe hollow spheres, $La_2(MoO_4)_3$ sphere superstructures composed of nanosheets,

* Corresponding author: e-mail: jiangwq@ustc.edu.cn

coralline-like ZnO and cube-shaped $CaSn(OH)_6$ were synthesized [14–17]. This method also can be used to synthesize $SrMoO_4$ particles with controllable nanostructure. Mao [18] and his colleagues have synthesized spherical $SrMoO_4$ assembled with nanosheets in an ulsonic bath. Very recently, spindle $SrMoO_4$ also have been reported by this method. In comparison to the most of the reported method, sonochemisty is facile for large scale fabrication, which enables it widely used in practical application. Moreover, $SrMoO_4$ particles can be suspended into insulating liquid to prepare electrorheological fluid (ERF), whose rheological properties are controlled by application of an external electric field. It is reported that the ER property is highly dependent on the microstructure of dispersing particles [19]. To this end, more work should be done to study the morphology controllable synthesis of $SrMoO_4$ particles by using the sonochemical method and investigate their ER properties.

In this work, a facile and fast sonochemical route was introduced to prepare $SrMoO_4$ crystals with hierarchical structure. The concentration of the reagent, the pH value, and surfactant has great influences on the morphologies of products. By varying the experimental conditions, $SrMoO_4$ with different morphologies, such as chrysanthemum-like, spindles, peanuts, spheres, and rods, can be obtained. Based on the experiments, a possible formation mechanism was proposed. The productivity is relatively high and the as-prepared chrysanthemum-like can be successfully used to prepare ER fluids. At last, the electrorheological property of product was investigated and its electric field-dependent shear viscosity was studied.

2 Experimental

2.1 Synthesis of the $SrMoO_4$ All the reagents were of analytical purity and used without further purification. In a typical synthesis, $SrCl_2{\cdot}6H_2O$ (5 mmol) were firstly dissolved in 50 mL distilled water to form solution 1. Then, $Na_2MoO_4{\cdot}2H_2O$ (5 mmol) and 5 mmol cetyltrimethylammonium bromide (CTAB) were dissolved in 50 mL distilled water to form solution 2. Under the ultrasound irradiation, the two solutions were mixed rapidly and irradiated in ambient air for 20 min. The ultrasound irradiation was accomplished with an ultrasonic cleaner (from Kesheng. Co., China, KS-120D) and the ultrasonic power is 120 W. Finally, a white precipitate was obtained. Before drying in a vacuum at 50 °C for 12 h, the precipitate was separated by centrifugation, washed with distilled water. The final products were characterized by X-ray powder diffraction (XRD), scanning electron microscopy (SEM), transmission electron microscopy (TEM) and selected-area electron diffraction (SAED).

2.2 Preparation of the ER fluid and testing of its ER effects The obtained $SrMoO_4$ samples were further dried at 120 °C for 2 h and then dispersed into silicone oil (density of $\sim$0.96 g cm^{-3}, viscosity of 500 cPa·s at 25 °C) by mechanical stirring to form a uniform electrorheological fluid (ERF). The volume fraction of $SrMoO_4$ particles was 20%. A rotational rheometer [20–22] (Physica, MCR 301, Anton Paar, Austria, the gap between the outer barrel and the inner probe was 0.42 mm) with the ER HVS/ERD180 and CC10-E accessory were used to measure the rheological characteristics of the ERF, where the ERF was placed into the barrel in between the two concentric circles.

2.3 Characterization X-ray powder diffraction (XRD) patterns were collected on a Philips X'pert Pro Super X-ray diffractometer with Cu Kα radiation ($\lambda = 1.5418$ Å). The morphology and size of the as-prepared products were observed by scanning electron microscope (SEM, Sirion 200) measurements. Transmission electron microscopy (TEM) and selected-area electron diffraction (SAED) were measured on a JEM-2100F, using an accelerating voltage of 200 kV.

3 Results and discussion

3.1 Structures and characterization The morphology of the obtained $SrMoO_4$ products synthesized via a facile sonochemical method is characterized by SEM and TEM. As shown in figure 1a, it clearly reveals that products consist almost entirely of micrometer-scale structures with uniform sizes and well-defined hierarchical chrysanthemum-like structure. The chrysanthemum-like particle is composed of several petals and its diameter is about 3 μm. Figure 1b shows that the surface of an individual flowerlike particle is composed of nanoparticles and then form spindle petal, finally built on the flower via oriented attachment. Figure 1c shows the TEM image of an individual particle. The SEM and TEM images indicate the as-prepared particle show a hierarchical nanostructure. Figure 1d and e are high resolution TEM image and SAED pattern, which reveal that as-synthesized $SrMoO_4$ particle is well crystallized. The SAED pattern shows regular diffraction spots, which suggests their

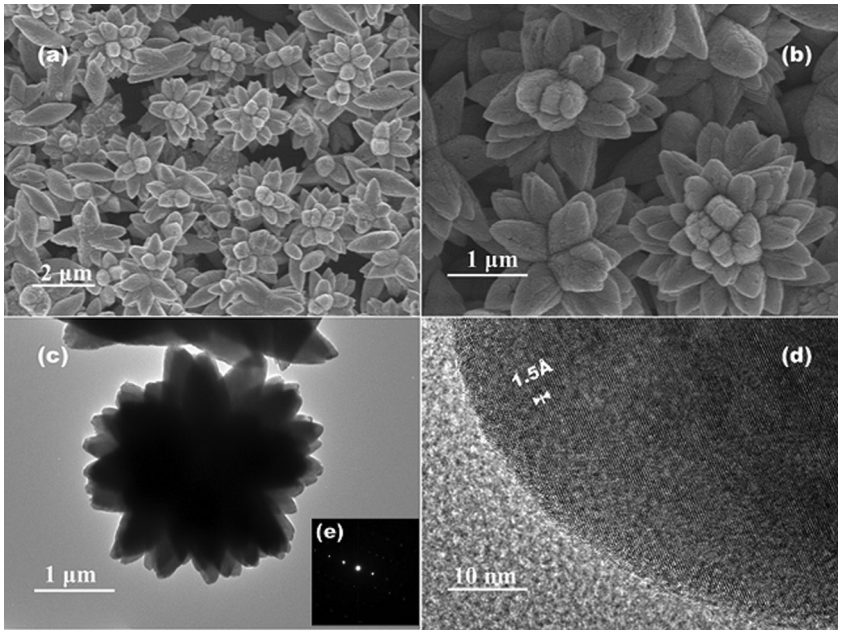

Fig. 1 Morphologies of $SrMoO_4$ samples obtained at 0.05 mol/L: (a) A typical SEM image, (b) a higher-magnification SEM image, (c) a typical TEM image, (d), (e) HRTEM image and the SAED pattern.

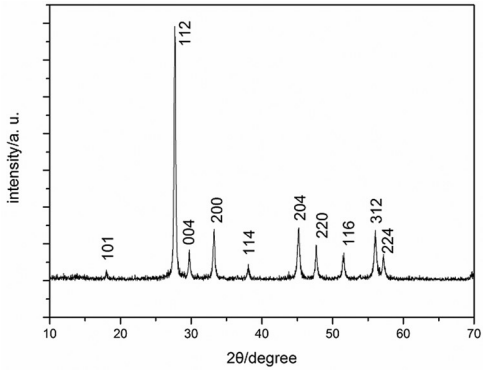

Fig. 2 XRD pattern of the obtained $SrMoO_4$ sample.

good crystallinity. From the HRTEM image, we can also find that the product is structurally uniform with an interplanar spacing of about 1.5 Å, which corresponds to the (008) lattice spacing of $SrMoO_4$.

To further studied the crystalline phase of the product, XRD characterization is employed. Figure 2 shows the XRD pattern of the as-synthesized products. The strong and sharp diffraction peaks show the good crystallization of the sample, which is consistent well with the SAED pattern. All diffraction peaks of the product can be indexed to the tetragonal system with the lattice constants a = 5.394 Å and c = 12.02 Å, which are in good agreement with the JCPDS card number 08–0482. No peaks of any other phases are detected, indicating the high purity of the product.

3.2 Effect of concentration The concentration of the chemical reagent has a great effect on the morphologies of the final $SrMoO_4$ products. In this work, several comparing reactions were operated to investigate their influence. The morphologies of them were observed with SEM, as shown in figure 3. A series of contrastive experiments were done and indicated that the concentration of reagent significantly affect the morphology of the $SrMoO_4$ .The crystallization was repeated at lower and higher concentrations (0.01, 0.1 and 0.5 mol/L, as compared with the standard of 0.05mol/L. Figure 3a shows the SEM image of the $SrMoO_4$ particles which is prepared under the 0.01 mol/L [Sr^{2+}]. It is very clear that all the particles show a flowerlike morphology. In

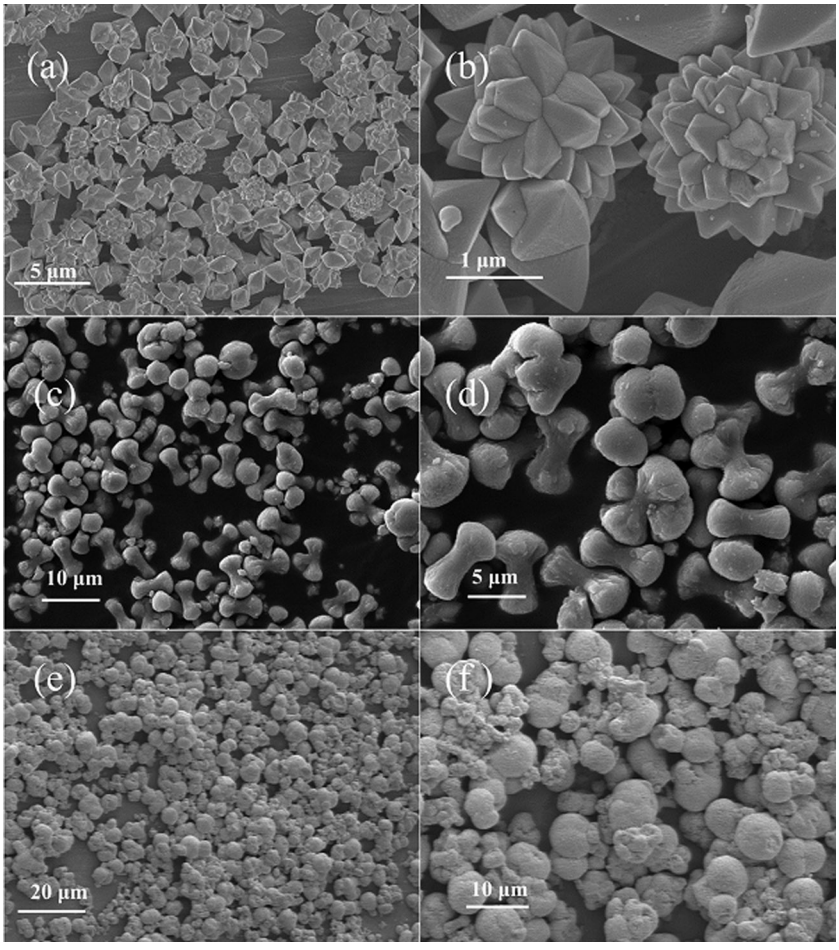

Fig. 3 SEM images and higher-magnification SEM images of samples obtained at (a), (b) 0.01 mol/L, (c), (d) 0.1 mol/L, (e), (f) 0.5 mol/L.

comparison to the chrysanthemum-like particles, these $SrMoO_4$ were composed of polyhedrons with distinct edge and face (figure 3b). When the concentration is increased to 0.05 mol/L, chrysanthemum-like particles were obtained (figure 1). With further increasing of the concentration to twice of the standard value, bone shaped products were obtained. As shown in figure 3c, the bonelike particles are sized about 2 μm in width and 7 μm in length. The two ends of particle were inflated and its surface was very rough (figure 3d). When the concentration was increased to 0.5 mol/L, only spherical particles were achieved (figures 3e and f). In this work, with increasing of the concentration, the $SrMoO_4$ particles tended to grow at ends and orient attachment towards spheres gradually.

3.3 Effect of pH value The pH value of reaction system is also one of the influence factors. To investigate the influence of pH value on the morphology, the $SrMoO_4$ was prepared at different pH values. When no acids and bases were added in the reaction, the pH value was 6. We used 0.1 M HCl and 0.1 M NaOH to adjust the pH of reaction system. In this work, the $SrMoO_4$ particles can keep their chrysanthemum-like nanostructure when the pH value was maintained between 6 and 11, as shown in figures 4b–d. However, when the pH value was decreased to 4, the morphology had drastic change and wire-like nanostructure was obtained. Figure 4a shows the SEM image of the products obtained at pH 4, which indicates all the particles are nanowires and their widths are several hundred nanometers and the lengths are several micrometers. It can be seen that, with the decrease of pH value, the dimension of the product decreased and the morphology changed from 3D flower to 1D nanowire.

The pH value influences the $SrMoO_4$ morphology by controlling the state of the Mo ions. The balance of different molybdate ions dependent on pH was shown as follows [23]. It has an equilibrium between MoO_4^{2} and $Mo_7O_{24}^{6-}$. When pH is higher than 6, there are massive MoO_4^{2} ions, which are enough for the formation

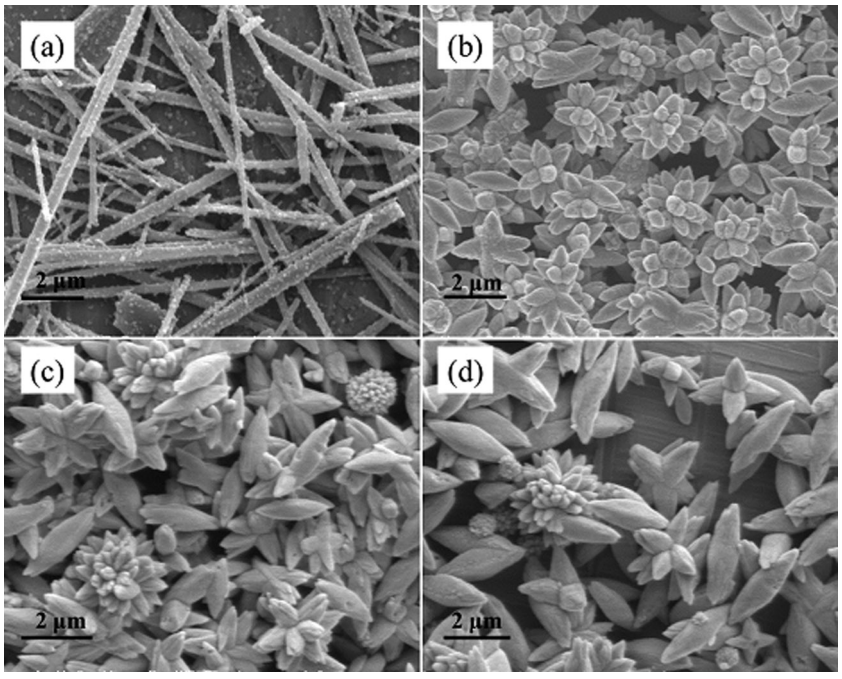

Fig. 4 SEM images of samples obtained at different pH (a) pH 4, (b) pH 6, (c) pH 9, (d) pH 11.

of tiny $SrMoO_4$ crystalline nuclei and growth of crystal. However, when pH is under 6, the concentration of the MoO_4^{2-} ions is relative low and they can be continuously released because of the presence of the $Mo_7O_{24}^{6}$ ions. The released MoO_4^{2-} anions combine with Sr^{2+} cations to give $SrMoO_4$ crystal nucleus. According to the well-known Gibbs-Thomson law, large particles grow at the cost of the smaller ones due to the difference in solubility. These tiny $SrMoO_4$ nanoparticles re-dissolve and grow along preferred orientation to form nanowires in the sonochemical process.

$$Mo_7O_{24}^{6-} \underset{pH<6}{\overset{pH\geq 6}{\rightleftharpoons}} MoO_4^{2-} + Sr^{2+} \rightarrow SrMoO_4$$

3.4 Effect of surfactants Surfactant-assistant synthesis has been a popular method to achieve morphological control. When no surfactant was added to the solution, the morphology of sample was spindles. Figure 5a shows the SEM image of the as-synthesized $SrMoO_4$ particles, which clearly indicate all the products show a typical spindle like nanostructure. The average size of the $SrMoO_4$ particles is about 3 μm. When CTAB (0.05 mol/L) is added into the reaction system, chrysanthemum-shaped microparticles are obtained (figure 1a). In this work, if the sodium dodecyl sulfate (SDS) was used to substitute the CTAB, the as-formed $SrMoO_4$ particles also show a hierarchical flowerlike structure (figure 5b). However, in comparison to the microparticles obtained in the presence of CTAB (figure 1a), those materials obtained in the SDS system are relatively loose and non-uniform. When 2 wt % polyacrylamide (M. W. 3,000,000) was used in the reaction, rod-like particles with length of ca. 3 μm were formed. However, as show in figure 5c, besides the micro-rods, some large spherical $SrMoO_4$ particles are also existed. When the rate of polyacrylamide is increased to 60 wt%, only spheres with 5–10 μm in diameter are achieved (figure 5d). Maybe the viscosity of polyacrylamide prevents the anisotropic growth of particles. Therefore, surfactants play an important role in the formation of the $SrMoO_4$ morphology.

3.5 Possible growth mechanism On the basis of the experimental results, a possible formation mechanism was proposed [11,18,24–26]. When the solution contained of MoO_4^{2-} and CTAB was placed in a sonicator, the ultrasound wave caused the formation of vesicle. Sr^{2+} was added to the above system under stirring and reacted with MoO_4^{2-} in the vesicle subsequently. Tiny $SrMoO_4$ spherical particles were produced as a consequence of homogeneous nucleation in the system. In thermodynamically, surface free energy of different crystal faces can be changed by surfactants. Ultrasound irradiation caused acoustic cavitation and promoted the formation of

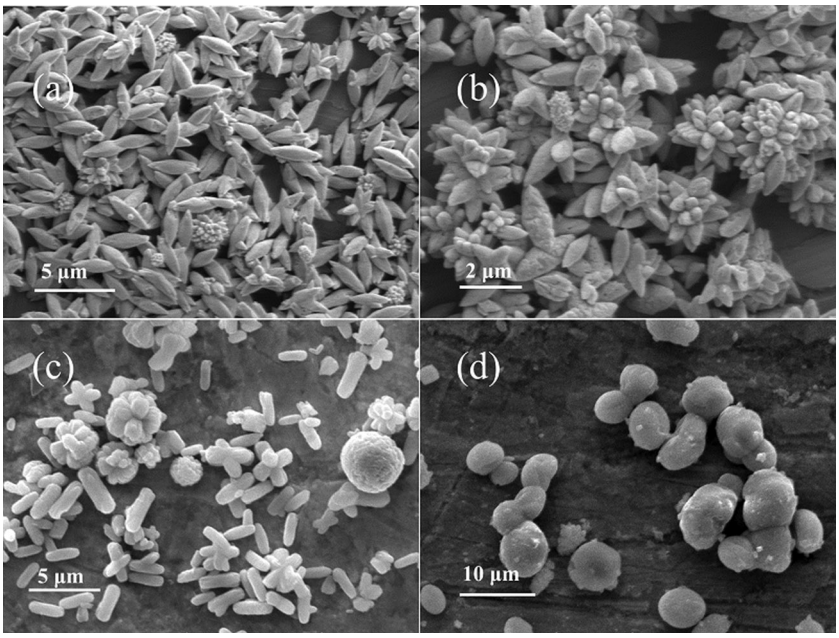

Fig. 5 SEM images of samples prepared with different surfactants: (a) no surfactant, (b) SDS, (c) polyacrylamide (2% w.t.),(d) polyacrylamide(60% w.t.).

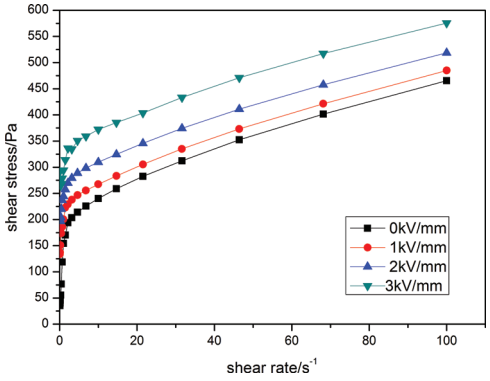

Fig. 6 The flow curves of shear stress versus shear rate under different applied electric field.

products. During the sonication progress, tiny $SrMoO_4$ crystalline particles oriented connected between adjacent particles and grew along preferred orientation. Due to the anisotropy of nuclei and selective adsorption of CTAB on the crystal facets, spindles with many ends were formed by orienting attachment and hierarchical chrysanthemum-shaped particles were obtained finally. The similar oriented attachment has been reported in synthesizing peanutlike $FeCO_3$ [27] and pomponlike $La_2(MoO_4)_3$ [15]. It can be concluded that surfactants and ultrasound irradiation play a very important role in the formation progress.

3.6 Electrorheological properties of as-prepared $SrMoO_4$ suspension Electrorheological fluid (ERF) is a kind of smart suspensions consisting of high dielectric particles dispersed in insulating liquid. The properties of ERF can be easily controlled by application of an external electric field [28]. Under applied electric filed, viscosity of ERF can increase rapidly due to the transforming from disordered to ordered of particulate phase. ERFs are generally considered to have many important applications in the automotive industry. In this work, the rheological behaviors of suspensions which were composed of $SrMoO_4$ particles suspended in silicone oil were also studied.

Figure 6 shows the flow curves of shear stress versus shear rate for the $SrMoO_4$ suspension under different applied electric field. When the electric field is applied, the suspension exhibits a strong increase in the shear

stress. It can be found that the suspensions exhibited a shear stress that increases with the shear rate. When shear rate increase to 100 s^{-1}, shear stress of the as-prepared ERF can be increased to as high as 600 Pa. Under the same shear rate, shear stress was increased with the increase of electric field strength and the maximum was obtained at 3 kV/mm. The shear stress obtained at 3 kV/mm was nearly twice higher than that obtained at 0 kV/mm.

4 Conclusion

In this work, a simple and efficient sonochemical method was developed for the synthesis of $SrMoO_4$ with hierarchical structure. $SrMoO_4$ with different morphologies, such as chrysanthemum-like, spindles, peanuts, spheres, and rods, can be obtained and the formation mechanism was discussed. The as-prepared chrysanthemum-like can be successfully used to prepare ER fluids and the electrorheological property of product was investigated. From the testing curve, it can be found that the shear stress is highly dependent on the electric field and it reaches to 600 Pa at 3 kV/mm, when the shear rate is increased to 100 s^{-1}.

Acknowledgements Financial supports from the National Natural Science Foundation of China (Grant No. 11125210) and the National Basic Research Program of China (973 Program, Grant No. 2012CB937500) are gratefully acknowledged.

References

[1] H. H. Yu, Z. Li, A. J. Lee, J. Li, H. J. Zhang, J. Y. Wang, H. M. Pask, J. A. Piper, and M. H. Jiang, Opt. Lett. **36**, 579 (2011).
[2] Q. O. Wei and D. H. Chen, Cent. Eur. J. Phys. **8**, 766 (2010).
[3] A. Radetinac, K. S. Takahashi, L. Alff, M. Kawasaki, and Y. Tokura, Appl. Phys. Express **3**, 073003 (2010).
[4] L. I. Ivleva, N. S. Kozlova, and A. V. Kir'yanov, Laser Phys. **20**, 635 (2010).
[5] Y. Liu, P. Yu, D. Q. Xiao, Y. F. Tian, X. Liu, and W. Q. Guo, Ferroelectrics **382**, 22 (2009).
[6] J. H. Bi, L. Wu, Y. F. Zhang, Z. H. Li, J. Q. Li, and X. Z. Fu, Appl. Catal. B-Environ. **91**, 135 (2009).
[7] B. C. Zhao, Y. P. Sun, S. B. Zhang, W. H. Song, and J. M. Dai, J. Appl. Phys. **102**, 113903 (2007).
[8] D. Y. Kim, J. S. Kim, B. H. Park, J. K. Lee, S. Y. Maeng, and S. J. Yoon, Integr. Ferroelectrics **67**, 25 (2004).
[9] T. Thongtem, A. Phuruangrat, and S. Thongtem, J. Nanopart. Res. **12**, 2287 (2010).
[10] Y. Sun, C. Li, L. Wang, X. Ma, Z. Zhang, M. Song, and P. Ma, Cryst. Res. Technol. **46**, 973 (2011).
[11] Y. Mi, Z. Y. Huang, F. L. Hu, Y. F. Li, and J. Y. Jiang, J. Phys. Chem. C **113**, 20795 (2009).
[12] Y. Sun, J. F. Ma, X. H. Jiang, J. R. Fang, Z. W. Song, C. Gao, and Z. S. Liu, Solid State Sci. **12**, 1283 (2010).
[13] K. S. Suslick, M. M. Fang, and T. Hyeon, J. Am. Chem. Soc. **118**, 11960 (1996).
[14] J. J. Zhu, S. Xu, H. Wang, J. M. Zhu, and H. Y. Chen, Adv. Mater. **15**, 156 (2003).
[15] Y. H. Ding, C. Y. Li, and R. Guo, Ultrason. Sonochem. **17**, 46 (2010).
[16] E. Kowsari, J. Nanopart. Res. **13**, 3363 (2011).
[17] S. G. Meng, D. Z. Li, M. Sun, W. J. Li, J. X. Wang, J. Chen, X. Z. Fu, and G. C. Xiao, Catal. Commun. **12**, 972 (2011).
[18] C. J. Mao, J. Geng, X. C. Wu, and J. J. Zhu, J. Phys. Chem. C **114**, 1982 (2010).
[19] J. B. Yin, X. P. Zhao, L. Q. Xiang, X. Xia, and Z. S. Zhang, Soft Matter **5**, 4687 (2009).
[20] W. H. Li, H. J. Du, G. Chen, S. H. Yeo, and N. Q. Guo, Rheol. Acta **42**, 280 (2003).
[21] W. H. Li, H. Du, and N. Q. Guo, Mat. Sci. Eng. A-Struct. **371**, 9 (2004).
[22] W. H. Li and X. Z. Zhang, Smart Mater. Struct. 035002 (2010).
[23] Y. M. Zhang, F. D. Yang, J. Yang, Y. Tang, and P. Yuan, Solid State Commun. **133**, 759 (2005).
[24] A. Cameirao, R. David, F. Espitalier, and F. Gruy, J. Cryst. Growth **310**, 4152 (2008).
[25] D. Chen, K. B. Tang, F. Q. Li, and H. G. Zheng, Cryst. Growth Des. **6**, 247 (2006).
[26] M. Brunsteiner, A. G. Jones, F. Pratola, S. L. Price, and S. J. R. Simons, Cryst. Growth Des. **5**, 3 (2004).
[27] S. Xuan, L. Hao, W. Jiang, L. Song, Y. Hu, Z. Chen, L. Fei, and T. Li, Cryst. Growth Des. **7**, 430 (2007).
[28] J. B. Yin and X. P. Zhao, Chem. Phys. Lett. **398**, 393 (2004).

